NORSAR Scientific Report No. 1-2009

Semiannual Technical Summary

1 July - 31 December 2008

Frode Ringdal (ed.)

Kjeller, February 2009

6   Summary of Technical Reports / Papers Published

6.1   Infrasound signals generated by atmospheric explosions in Finland as observed at the ARCES seismic array and microbarograph mini-array (sponsored by US Army Space and Missile Defence Command, Contract no. W9113M-05-C-0224)

6.1.1 Introduction

The Finnish military destroys expired ammunition at a site in northern Lapland in a sequence of explosions every year between August and September. Each explosion has a yield of approximately 20000 kg and the seismic signals recorded at the ARCES array in northern Norway indicate a magnitude of approximately 1.5. The events have been of great interest due to the generation of infrasound signals which have been recorded on the seismic traces at ARCES and by both seismic and microbarograph instruments at Apatity (Vinogradov and Ringdal, 2003; Gibbons et al., 2007). These explosions provide very useful reference events for infrasound sources since the location is known (67.934^{o}N, 25.832^{o}E: see Figure 6.1.1) and the origin times are very tightly constrained by the seismic observations. It now appears that infrasound from these events can be observed at far greater distances than previously assumed with signals likely to come from these sources being observed at the IMS infrasound arrays I18DK (Qaanaaq, Greenland) and I26DE (Freyung, Germany) making the events useful for studies of long-distance sound propagation (Bahavar et al., 2008).
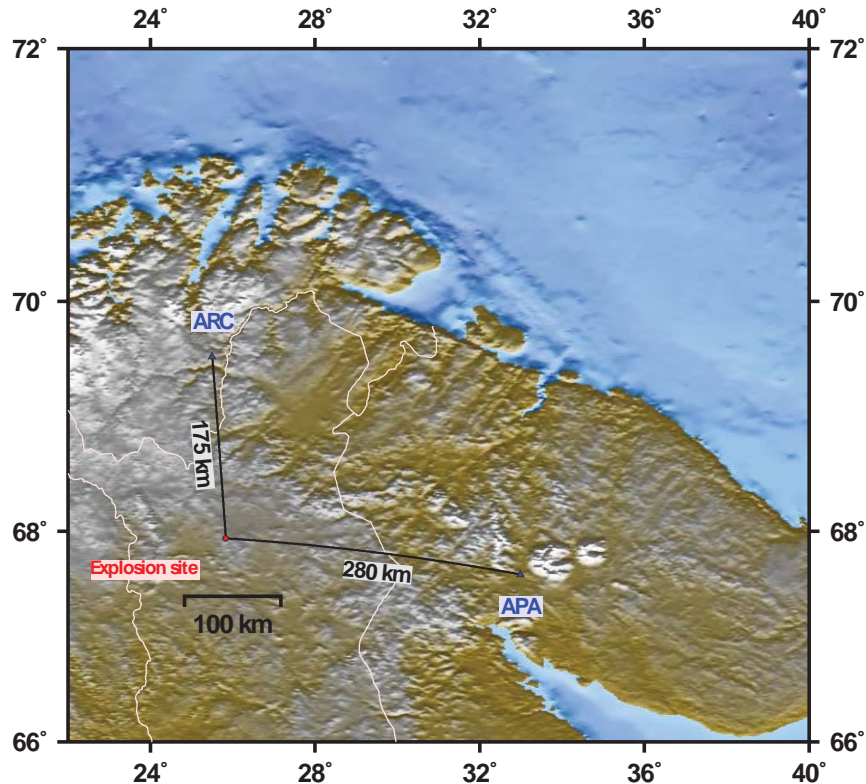

Fig. 6.1.1.   Location of the Finnish explosion site (67.934^{o}N, 25.832^{o}E) in relation to the arrays at ARCES and Apatity.

The fall of 2008 was no exception with a total of 36 explosions being conducted between August 13 and September 11 (see Table 6.1.1). As in previous years, a very high degree of similarity was observed between the seismic signals from the events allowing them all to be detected with an essentially zero false alarm rate using a multichannel correlation detector (Gibbons and Ringdal, 2006).

The 2008 explosion sequence has been of special interest since an experimental 3-site array of microbarographs deployed within the ARCES array (Roth et al., 2008) has allowed for a direct comparison of the infrasound signals recorded on the seismometers and those recorded on co-located microbarographs. Due to local planning restrictions (which have also delayed indefinitely the deployment of the IMS infrasound array IS37) no wind noise reduction system has been allowed other than the use of porous hoses. A full description of the installation, including instrumentation and data samples, is provided by Roth et al. (2008), and preliminary data analysis is provided by Ringdal et al. (2008).

Table 6.1.1. Explosions at the Finnish military base in Lapland during 2008. UT Origin time estimates are provided rounded to the nearest second.

Date (day of year)		First event		Second event
13 Aug 2008 (226)	01	09.00.00	02	13.00.00
14 Aug 2008 (227)	03	09.00.00	04	13.00.00
15 Aug 2008 (228)	05	08.30.00	06	11.59.59
16 Aug 2008 (229)	07	08.30.00	08	11.30.00
17 Aug 2008 (230)	09	08.29.58	10	11.30.00
18 Aug 2008 (231)	11	06.59.59	12	13.59.58
19 Aug 2008 (232)	13	10.59.59		
20 Aug 2008 (233)	14	10.59.58		
21 Aug 2008 (234)	15	11.00.00		
22 Aug 2008 (235)	16	11.00.00		
23 Aug 2008 (236)	17	13.15.01		
24 Aug 2008 (237)	18	12.30.00		
25 Aug 2008 (238)	19	11.30.00		
26 Aug 2008 (239)	20	11.00.00		
27 Aug 2008 (240)	21	11.00.00		
28 Aug 2008 (241)	22	10.45.01		
29 Aug 2008 (242)	23	11.00.00		
30 Aug 2008 (243)	24	09.59.59		
31 Aug 2008 (244)	25	11.00.00		
1 Sep 2008 (245)	26	11.30.00		
2 Sep 2008 (246)	27	11.00.03		
3 Sep 2008 (247)	28	11.00.06		
4 Sep 2008 (248)	29	10.30.00		
5 Sep 2008 (249)	30	10.00.00		
6 Sep 2008 (250)	31	11.00.00		
7 Sep 2008 (251)	32	09.29.59		
8 Sep 2008 (252)	33	09.29.59		
9 Sep 2008 (253)	34	09.29.59		

Table 6.1.1. Explosions at the Finnish military base in Lapland during 2008. UT Origin time estimates are provided rounded to the nearest second.

Date (day of year)		First event		Second event
10 Sep 2008 (254)	*35*	09.29.59		
11 Sep 2008 (255)	*36*	09.30.00		

6.1.2   Observations

Figure 6.1.2 displays the waveforms observed on co-located seismic and infrasound sensors at the ARA1 site of the ARCES array for each of the 36 events in 2008. The seismic traces in the left panel show the seismic P- and S- phases arriving 29 and 49 seconds respectively after each shot and also acoustic signals between 500 and 700 seconds. Whilst the acoustic phases are generally visible in the filtered data, they are of somewhat smaller amplitude than in some previous years. (Gibbons et al., 2007, display a corresponding plot for 2002 in which the amplitudes of the acoustic phases are frequently greater than those for the seismic phases.) An additional complication which has been particularly problematic for 2008 is the presence of unrelated seismic signals in the interval in which the acoustic phases are anticipated. Signals visible between 500 and 700 seconds after events 14, 15, 16, and 24 are very clearly regional or teleseismic signals unrelated to the explosions in Finland which may make the detection of acoustic phases at these times difficult or impossible.

The right hand panel of Figure 6.1.2 shows microbarograph data from the same site, for the same time intervals. The seismic arrivals are not visible in these waveforms. More often than not, the acoustic phases recorded on the seismic instruments are also visible with a significantly higher amplitude than the background noise. On other days, the background noise is very much higher and matches the amplitudes of the observed signals.

The only way to identify which parts of the waveforms truly correspond to acoustic signals from the direction of interest is to perform slowness analysis. We calculate cross-correlation coefficient traces between pairs of signals and then loop around a grid of slowness vectors and calculate the mean values for the corresponding time delays (c.f. Brown et al., 2002). If the slowness vector corresponding to the maximum average cross-correlation coefficient does not fall within limits appropriate for a wavefront propagating with air-sound speed from a plausible backazimuth then we have to assume that the observed signal is probably not an acoustic phase from one of our events. With the seismic sensors, we have traces from 25 sites and so can perform slowness analysis either with the full array or with one of many possible subsets of sensors. There are only three sensors in the infrasound subarray. Whilst it is possible to obtain reasonable slowness estimates if all three sensors record a signal well, there is no redundancy and should a single one of the sensors fail, or be subject to excessive noise, no direction estimate is possible.

We have restricted our analysis to frequency ranges 2.0 - 7.0 Hz for the seismic sensors and between 1.0 - 7.0 Hz for the microbarographs. For the seismic sensors, the limitation to frequencies above 2 Hz is due to the high amplitude microseismic noise at lower frequencies. The frequency range for the infrasound mini-array is the result of the sensor configuration. At low frequencies, there is no resolution in slowness-space and, at high frequencies, aliasing results in an ambiguity of direction estimates.
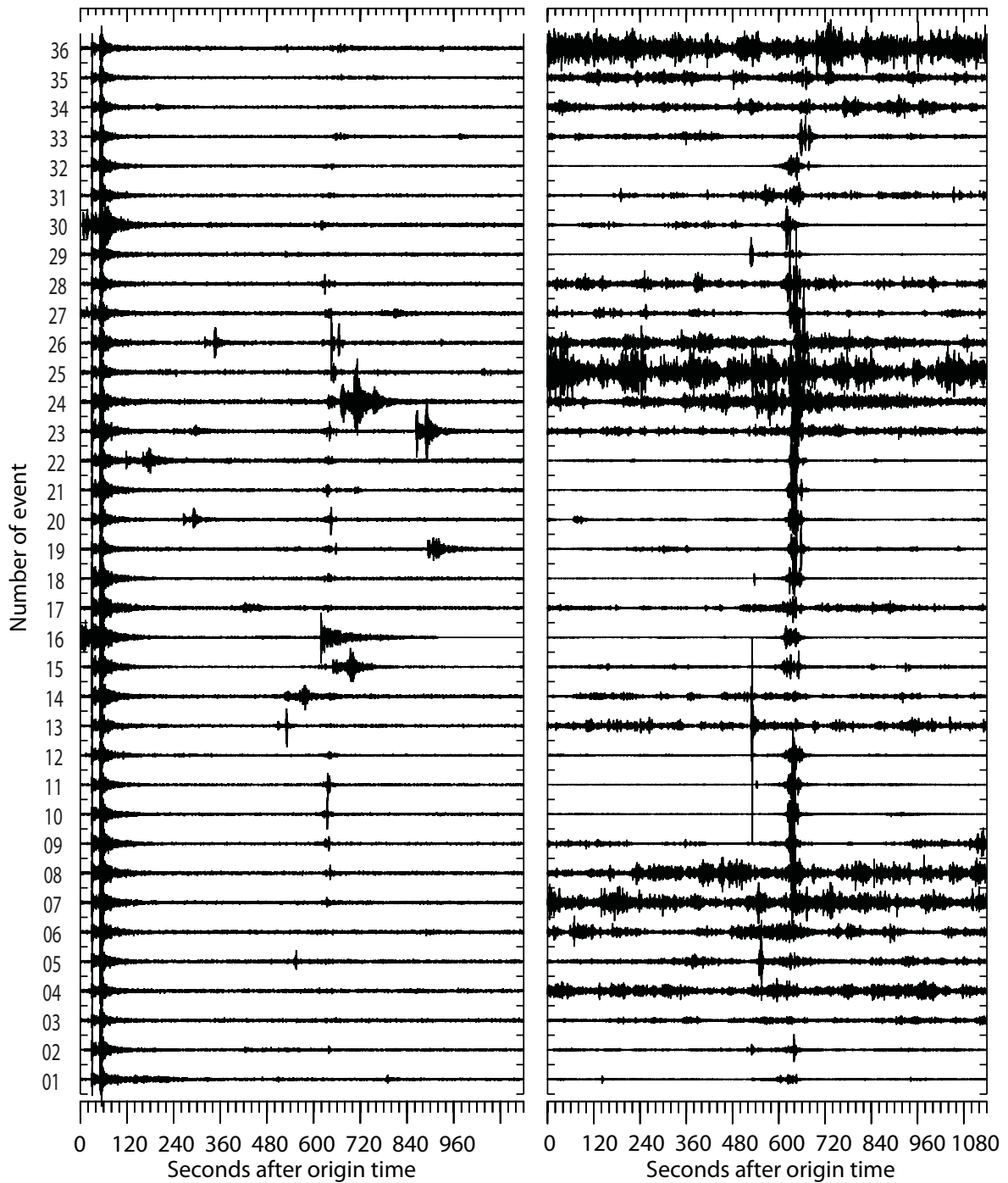
Fig. 6.1.2.   Waveforms from the short-period vertical seismic sensor ARA1_sz (left) and the co-
located microbarograph sensor ARA1_BDF (right) for the events as listed in Table 6.1.1.
The same vertical scale is applied to all of the seismic traces within each panel. All
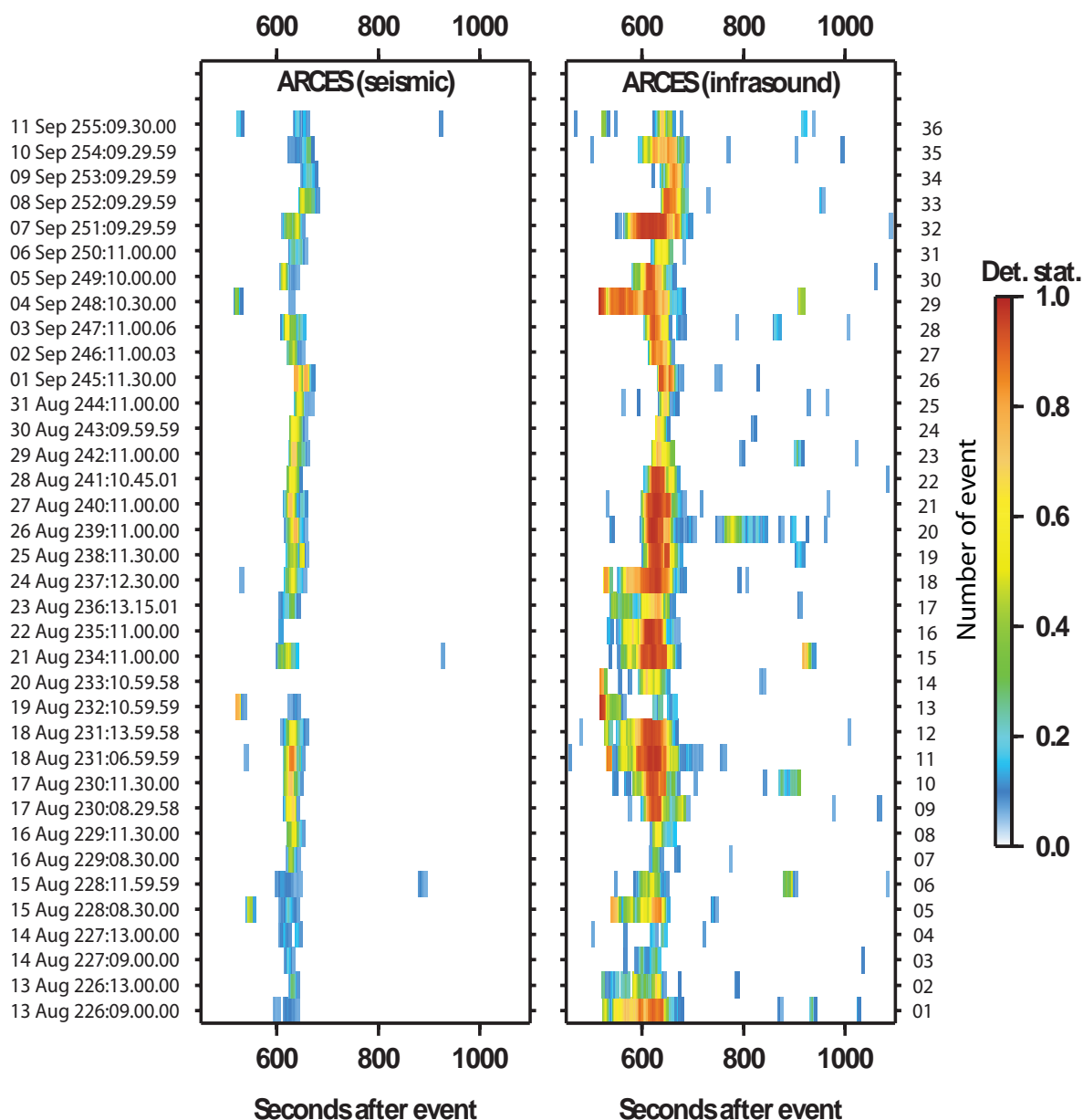waveforms are bandpass filtered between 2 and 7 Hz.

Fig. 6.1.3. *Each pixel represents the value of the detection statistic defined in Equation (15) of Brown et al. (2002) for a 10 second long data segment, bandpass filtered between 2.0 and 7.0 Hz, on the condition that the backazimuth and apparent velocity indicated by the cross-correlation analysis fell within the intervals [168º:190º] and [0.3 kms^{-1}:0.8 kms^{-1}] respectively. The time provided to the left is the event origin time.*

Figure 6.1.3 shows the value of the maximum mean cross-correlation coefficient as a function of time following the explosion on the condition that the preferred slowness-vector is consistent with an anticipated acoustic phase. All events appear to generate infrasound waves which are detected on both the seismic and infrasonic sensors with the exception of event 14 for which no observation is made on the seismometers. There is however a sound signal detected on the infrasound sensors at the anticipated time which suggests that the absence of a detection on the seismic sensors is indeed caused by interference from unrelated seismic signals.

One feature which has not previously been observed in recordings from these events is the presence of acoustic phases with higher apparent velocities between around 800 and 950 seconds. They are detected only marginally for three events (6, 15, and 36) on the seismic sensors, but are clearly visible on the microbarograph data for several more.

ARCES seismic sensors (A0, A-ring, B-ring)   ARCES infrasound sensors (ARA1, ARA2, ARB2)
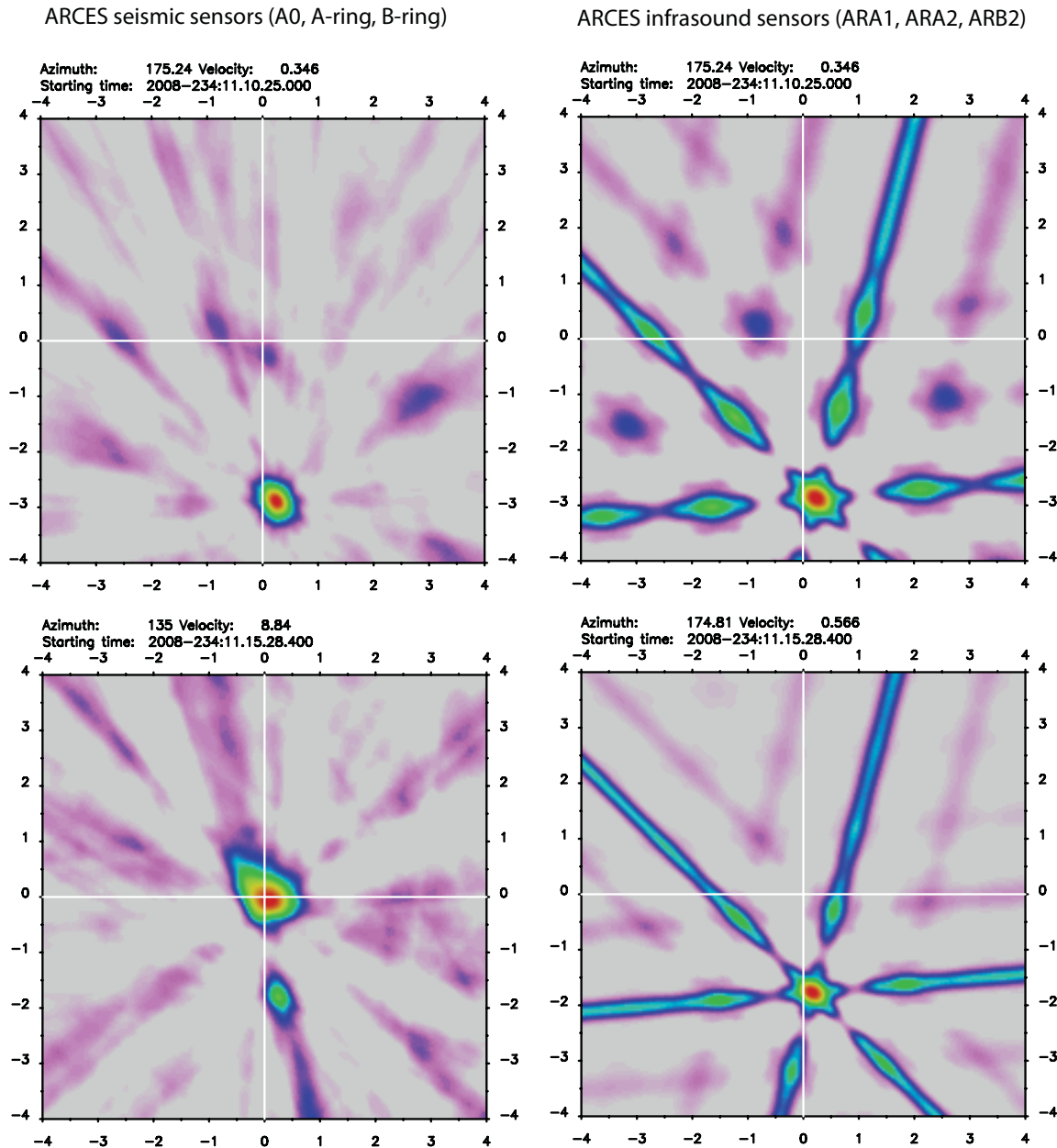

Fig. 6.1.4.   Slowness estimates at 625 seconds (above) and 928 seconds (below) after the explosion at 11.00 UTC on August 21, 2008. For the seismic estimates, only the innermost nine sites of the ARCES array are used. The seismic estimate for the later arrival (lower left panel) indicates an apparent velocity consistent with seismic wave speed, although evidence is seen for energy arriving with sound speed.

Examples of direction estimates, both for a typical phase in the 500-700 second interval and for one of the newly observed phases between 800 and 950 seconds, are shown in Figure 6.1.4.

The significantly higher apparent velocity for the later arrival is consistent with a steeper angle of incidence as would be anticipated for a thermospheric arrival. At a distance of 178 km, the range of travel times 800 to 950 seconds corresponds to celerities between 0.187 kms^{-1} and 0.223 kms^{-1}, which is comparable with the values plotted by Mutschlecner and Whitaker (1999) for thermospheric arrivals observed from explosions at the Nevada Test Site, observed at a distance of approximately 210 km.
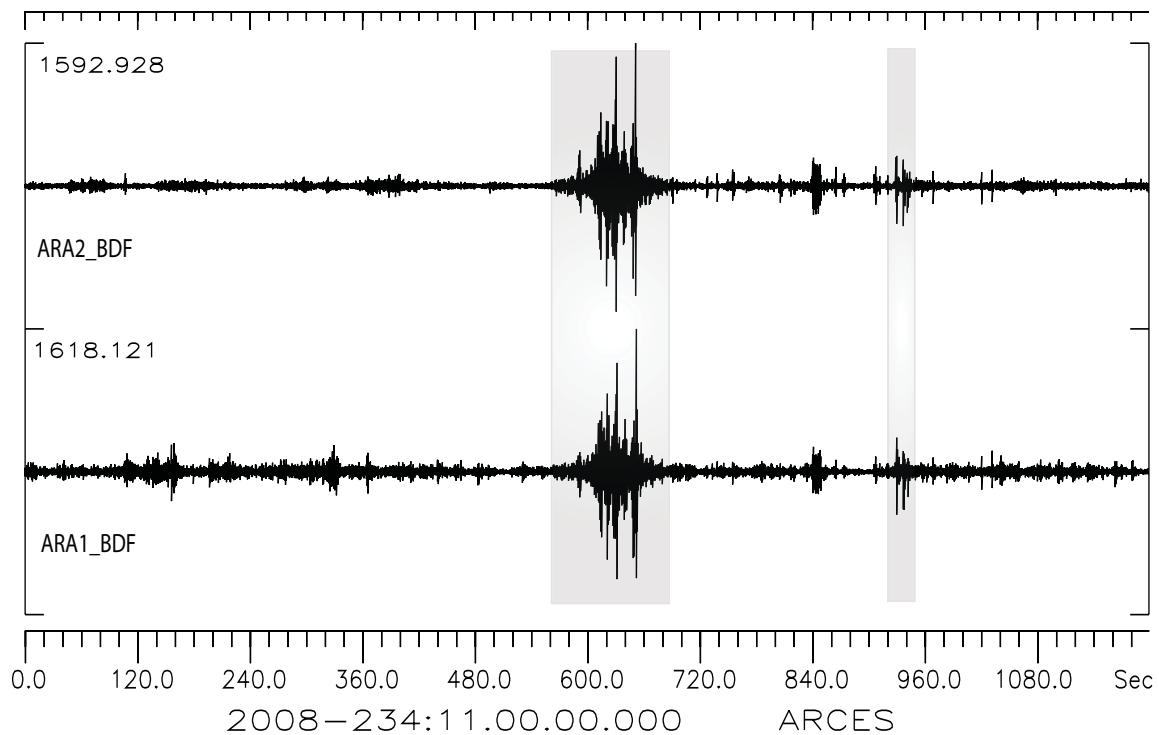

Fig. 6.1.5.   Traces of ARCES microbarograph data following the 11.00 UT explosion on August 21, 2008. The grey boxes indicate the time-periods for which the slowness analysis indicates a sound wave from the appropriate direction. All features in this data interval which are not covered by the grey boxes are not consistent with presumed acoustic arrivals from the explosion.

An example of the waveforms corresponding to the two types of arrival is displayed in Figure 6.1.5. In this plot, and in corresponding plots for other events in the sequence, the presumed thermospheric arrival is both of lower amplitude and shorter duration than the presumed strato-spheric arrivals. The longer duration signal appears to be rather continuous in nature whereas the presumed thermospheric arrival appears to consist of very short duration bursts. This would also appear to be consistent with the observations of Whitaker and Mutschlecner (2008) and may contribute to the poorer detection rate since the cross-correlation method is best suited to long duration, coherent signals.
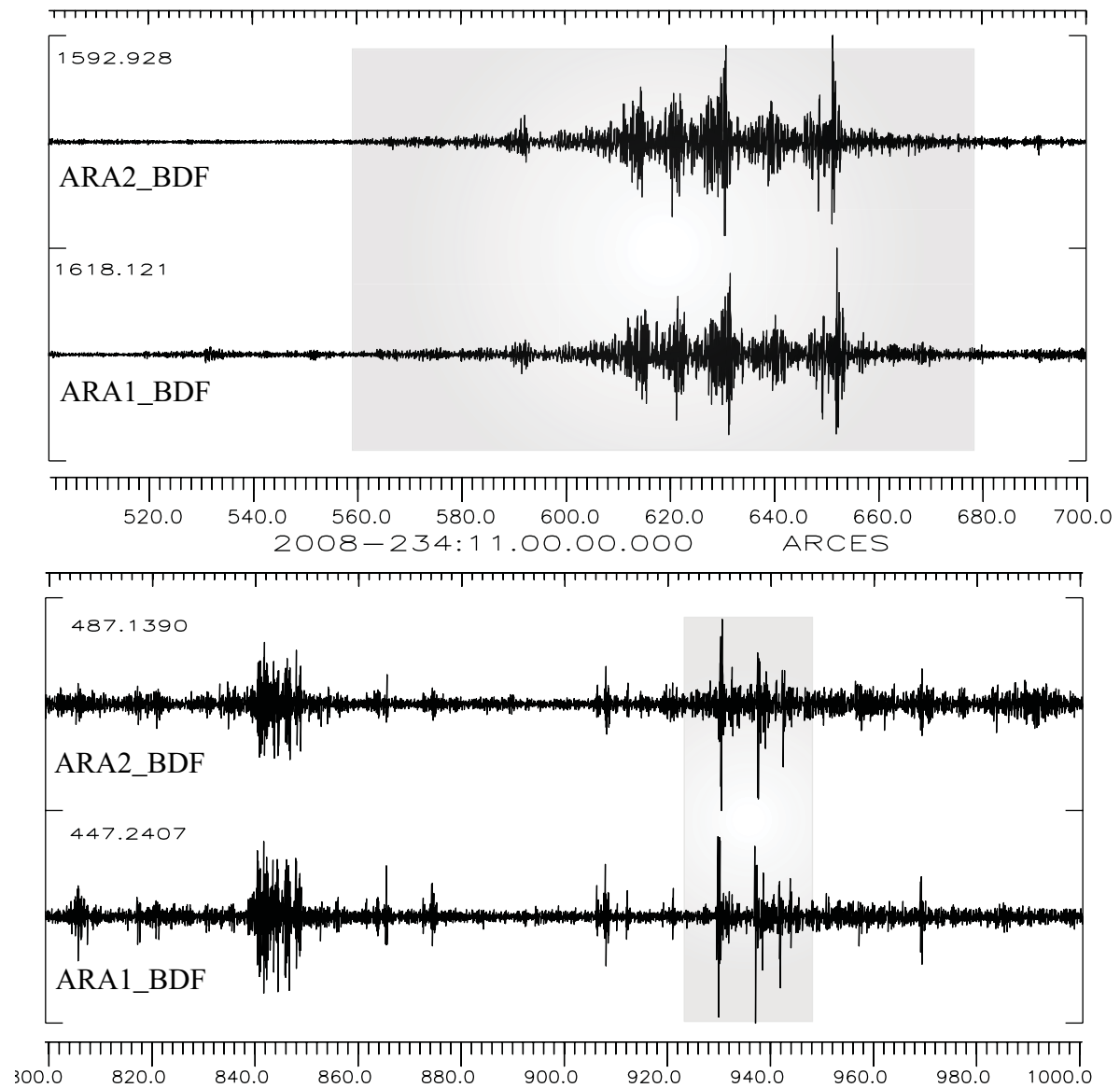
Fig. 6.1.6. Time in seconds following the explosion at 11.00 UT on August 21, 2008, as recorded on the ARA2_BDF and ARA1_BDF microbarograph channels at ARCES. Both panels are 200 second long enlargements of the waveforms displayed in Figure 6.1.5.

6.1.3   Summary

We present the origin times of 36 explosions which took place during August and September 2008 at a site in northern Finland (coordinates 67.934°N, 25.832°E). The explosions this year are the first to be recorded by the microbarograph mini-array within the ARCES seismic array at a distance of approximately 178 km. Acoustic signals were detected on the microbarograph sensors following every one of the explosions and on the seismic sensors following all but one. The non-detection in this case is attributed to an unrelated seismic signal arriving in the interval in which the acoustic arrival is anticipated.

Whilst the seismic array has served well as a surrogate infrasound array for these and other seismo-acoustic and infrasound events, this field deployment has demonstrated that the microbarograph sensors are essential to capture low amplitude infrasound signals which are too weak to be registered on the seismic sensors. Comparing the left and right panels of Figure 6.1.3 it is clear that the onset of the infrasound phases inferred from the microbarograph array is often significantly earlier than for the seismic sensors. A closer inspection of many of the presumed stratospheric returns (c.f. upper panel of Figure 6.1.6) reveals that many of the signals have quite long durations and are quite emergent in nature. This is significant for the validation of models for atmospheric sound propagation since the onset time inferred from the seismic traces (only sensitive to the highest amplitudes) may be 30-60 seconds higher than the onset time estimated from the microbarograph data.

In addition to the phases identified by Gibbons et al. (2007), all arriving between 500 and 700 seconds after origin time, a number of additional arrivals have been detected between 800 and 950 seconds. These are associated with considerably higher apparent velocities, consistent with steeper angles of incidence which would be anticipated from thermospheric returns. The travel times are consistent with thermospheric arrivals observed from Nevada Test Site explosions recorded at the comparable distance of 210 km (Mutschlecner and Whitaker, 1999). There were only three such detections on the seismic sensors and all of these were quite marginal. There were 11 clear detections on the infrasound mini-array. This represents approximately 30% of the events which is similar to the observation rates quoted by Whitaker and Mutschlecner (2008). However, given that only a minimal wind noise reduction system (for noise protection) is available to us within the planning limitations at the ARCES site, it is not clear to what extent this is the result of an absence of the phases and to what extent this is due to excessive background noise[1]. It is clear that very local noise conditions apply and that an increase in the number of sensors would mitigate this problem.

The thermospheric arrivals appear to be of shorter duration and of lower amplitude than the presumed stratospheric returns. This will contribute to their non-detection on the seismic sensors.

The deployment of more infrasound sensors would allow an examination of infrasound over a broader range of frequencies (mitigating the aliasing for high frequency signals and the lack of resolution for low frequency signals) and would make the detection procedure more robust by providing some redundancy among sensors.

---

1. The thermospheric arrival from the last event in Table 6.1.1 was observed clearly on one channel and barely observed on the other channels and was very nearly missed due to the low correlation values.

References

Bahavar, M., Barker, B. W., Bennett, T. J., Israelsson, H. G., Kohl, B. C., Kung, Y.-L., Murphy, J. R., and Oancea, V. (2008). Nuclear Explosion and Infrasound Event Resources of the SMDC Monitoring Research Program, in "*Proceedings of the 2008 Monitoring Research Review, Portsmouth VA, September 23-25, 2008: Ground-Based Nuclear Explosion Monitoring Technologies*" pp. 923-931. LA-UR-08-05261. https://www.nemre.nnsa.doe.gov/prod/researchreview/2008/PAPERS/07-01.PDF

Brown, D. J., Katz, C. N., Le Bras, R., Flanagan, M. P., Wang, J., and Gault, A. K. (2002). Infrasonic Signal Detection and Source Location at the Prototype International Data Centre, *Pure appl. geophys.*, **159**, pp. 1081-1125.

Gibbons, S. J. and Ringdal, F. (2006). The detection of low magnitude seismic events using array-based waveform correlation, *Geophys. J. Int.*, **165**, pp. 149-166.

Gibbons, S. J., Ringdal, F., and Kværna, T. (2007). Joint seismic-infrasonic processing of recordings from a repeating source of atmospheric explosions, *J. Acoust. Soc. Am.*, **122**, pp. EL158-EL164.

Mutschlecner, J. P., and Whitaker, R. W. (1999). Thermospheric Infrasound Signals, in "*Proceedings of the 21st Seismic Research Symposium, Las Vegas, NV, September 21-24, 1999: Technologies for Monitoring The Comprehensive Nuclear-Test-Ban Treaty*", Volume II, pp. 151-158. LA-UR-99-4700. https://www.nemre.nnsa.doe.gov/prod/researchreview/1999/papers5/mutschlecner_whitaker.pdf

Ringdal, F., Kværna, T., and Gibbons, S. J. (2008). Initial studies of signals recorded by ARCES infrasound sensors. *In NORSAR Scientific Report: Semiannual Technical Summary No. 2-2008, NORSAR, Kjeller, Norway.* pp. 60-85.

Roth, M., Fyen, J., and Larsen, P. W. (2008). Setup of an experimental infrasound deployment within the ARCES array. *In NORSAR Scientific Report: Semiannual Technical Summary No. 2-2008, NORSAR, Kjeller, Norway.* pp. 52-59.

Vinogradov, Y. and Ringdal, F. (2003). Analysis of infrasound data recorded at the Apatity array. *In NORSAR Scientific Report: Semiannual Technical Summary No. 1-2003, NORSAR, Kjeller, Norway.* pp. 68-77.

Whitaker, R. W. and Mutschlecner, J. P. (2008). A comparison of infrasound signals refracted from stratospheric and thermospheric altitudes, *J. Geophys. Res.*, **113**, D08117, doi:10.1029/2007JD008852.

S. J. Gibbons